Graphene Oxide Attenuates Th2-Type Immune Responses, but Augments Airway Remodeling and Hyperresponsiveness in a Murine Model of Asthma

Michael R. Shurin,[†] Naveena Yanamala,[‡] Elena R. Kisin,[‡] Alexey V. Tkach,[‡] Galina V. Shurin,[†] Ashley R. Murray,[‡] Howard D. Leonard,[‡] Jeffrey S. Reynolds,[‡] Dmirtiy W. Gutkin,[†] Alexander Star,[§] Bengt Fadeel,[⊥] Kai Savolainen,[△] Valerian E. Kagan,[∥] and Anna A. Shvedova[‡,#,*]

[†]Department of Pathology, University of Pittsburgh School of Medicine, Pittsburgh, Pennsylvania 15260, United States, [‡]Pathology & Physiology Research Branch/NIOSH/CDC, Morgantown, West Virginia 26505, United States, [§]Department of Chemistry, and [∥]Department of Environmental and Occupational Health, University of Pittsburgh, Pittsburgh, Pennsylvania 15260, United States, [⊥]Division of Molecular Toxicology, Institute of Environmental Medicine, Karolinska Institutet, 171 77 Stockholm, Sweden, [△]Nanosafety Research Center, Finnish Institute of Occupational Health, 02500 Helsinki, Finland, and [#]Department of Physiology and Pharmacology, West Virginia University, Morgantown, West Virginia 26505, United States

ABSTRACT Several lines of evidence indicate that exposure to nanoparticles (NPs) is able to modify airway immune responses, thus facilitating the development of respiratory diseases. Graphene oxide (GO) is a promising carbonaceous nanomaterial with unique physicochemical properties, envisioned for a multitude of medical and industrial applications. In this paper, we determined how exposure to GO modulates the allergic pulmonary response. Using a murine model of ovalbumin (OVA)-induced asthma, we revealed that GO, given at the sensitization stage, augmented airway hyperresponsiveness and airway remodeling in the form of goblet cell hyperplasia and smooth muscle hypertrophy. At the same time, the levels of the cytokines IL-4, IL-5, and IL-13 were reduced in broncho-alveolar lavage (BAL) fluid in GO-exposed mice. Exposure to GO during sensitization with OVA decreased eosinophil accumulation and increased recruitment of macrophages in BAL fluid. In line with the cytokine profiles, sensitization with OVA in the presence of GO stimulated the production of OVA-specific IgG2a and down-regulated the levels of IgE and IgG1. Moreover, exposure to GO increased the macrophage production of the mammalian chitinases, CHI3L1 and AMCase, whose expression is associated with asthma. Finally, molecular modeling has suggested that GO may directly interact with chitinase, affecting AMCase activity, which has been directly proven in our studies. Thus, these data show that GO exposure attenuates Th2 immune response in a model of OVA-induced asthma, but leads to potentiation of airway remodeling and hyperresponsiveness, with the induction of mammalian chitinases.

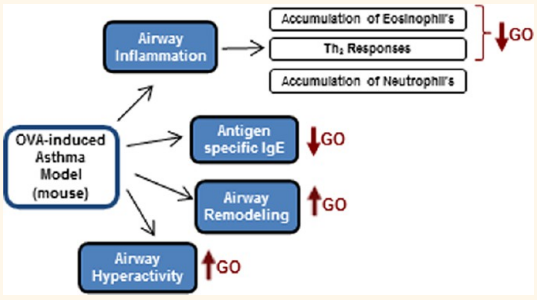

KEYWORDS: Th2 responses · macrophage activation · IgE-independent AHR · chitinases

Carbonaceous nanoparticles (CNPs) and their derivatives have been widely used for a number of applications, including energy storage devices, superconducting products, magnets, biologic materials, and catalysts. Numerous studies have focused on the toxicity issues associated with CNP exposure, while limited information is currently available regarding their immunomodulating potential. Growing evidence indicates that local inflammatory responses following CNP exposure can result in modified systemic immune reactivity.[1−3]

Pulmonary inflammation provides a broad spectrum of signals facilitating recruitment and/or activation of various immune cells, associated with release of chemokines, cytokines, growth factors, and "danger" signals. In allergic asthma, T helper 2 (Th2)-type lymphocytes play a major role in triggering inflammatory responses. Upon

* Address correspondence to ats1@cdc.gov.

Received for review December 17, 2013 and accepted May 21, 2014.

Published online May 21, 2014
10.1021/nn406454u

allergen sensitization, they release inflammatory cytokines, IL-4 and IL-13, both of which stimulate B cells to synthesize IgE, and IL-5 necessary for initiating eosinophilic inflammation,[4] while suppressing the Th1 type of immune responses.[5−8] Several CNPs, including carbon nanotubes and carbon black, potentiate the pulmonary allergic responses by stimulating Th2-mediated immunity.[9−12] While exposure to [Gd@C(82)(OH)(22)](*n*) nanoparticles stimulated Th1-type responses,[13] pulmonary exposure to multiwalled (MW) and single-walled (SW) carbon nanotubes (CNTs) has induced nonspecific suppression of proliferative responses of splenic T cells.[1,3,14] Furthermore, exposure to nanoparticles during allergen sensitization results in a significant decrease in both airway reactivity and Th2-type cytokines compared to animals treated with allergen alone, suggesting specific immunomodulatory properties of CNPs.[15] Taken together, these studies suggest that CNPs with different physical and chemical properties, such as surface area, charge, structure, and size, can facilitate allergic inflammation.[16−18]

A polysaccharide chitin, the second most abundant biopolymer in the world that can be found in the cell walls of fungi, microfilarial sheaths of helminths, and exoskeletons of insects and crustaceans, is emerging as a new important allergen.[19] Analysis of dust collected from the homes of asthmatic individuals revealed the presence of the chitin as environmentally widespread and associated with β-glucans, possibly from ubiquitous fungi.[20] This attracted significant attention to chitinases, hydrolytic enzymes that break down glycosidic bonds in chitin. Although mammals do not produce chitin, they have two functional chitinases (chitotriosidase CHIT1 and acidic mammalian chitinase CHIA/AMCase) as well as chitinase-like proteins (such as BRP-39/YKL-40) that have high sequence similarity but lack chitinase activity.[21] Human chitinases may be related to allergies, and asthma has been linked to enhanced chitinase expression levels.[22] Chitinase-3-like protein 1 (CHI3L1), also known as BRP-39 in mice or YKL-40 in humans, is a glycoprotein secreted by activated macrophages, chondrocytes, neutrophils, and synovial cells and is thought to play a role in the process of inflammation and tissue remodeling.[23,24] Chitinases might be involved in pathogenesis of different lung diseases, including asthma, COPD, sarcoidosis, pulmonary tuberculosis, pneumonia, and lung cancer.[25] However, it is unknown if chitinases might be affected by exposure to nanomaterials, especially during development of asthma.

In this paper, we evaluated how pulmonary exposure to graphene oxide (GO) nanoparticles altered immune responses, allergic pulmonary inflammation, airway remodeling, and airway hyperresponsiveness (AHR) in a murine model of ovalbumin (OVA)-induced allergic asthma. We assessed the effect of exposure to GO during both OVA sensitization and OVA challenge. We compared Th1/Th2 cytokine balance in bronchoalveolar lavage (BAL) fluid, serologic immunoglobulin profiles, and patterns of eosinophil, neutrophil, alveolar macrophage, and lymphocyte accumulation in the lungs in treated animals. We show that pulmonary GO administration significantly suppresses a classic Th2-polarized immune response and alters the pattern of inflammatory cell recruitment in the lungs. Despite diminished Th2-type response, we observed an increased airway remodeling and AHR in mice receiving OVA and GO during the sensitization phase. Finally, we revealed that the mechanism underlying augmented AHR is attributed to extended airway remodeling, at least in part, through the induction of mammalian chitinases by alveolar macrophages upon GO stimulation.

RESULTS

GO Given at Sensitization, But Not Challenge Phase, Promoted Airway Hyperresponsiveness. To evaluate airway responsiveness to direct stimulation, we utilized the methacholine challenge test and a whole body plethysmography. Administration of GO at the time of OVA sensitization (GO/SENT) (Figure 1) significantly increased airway responsiveness to methacholine as compared to control (PBS) and OVA-only treated mice (OVA/ALL) up to 2.5-fold ($p < 0.05$, Figure 2). Importantly, exposure to GO at OVA challenge (GO/CHAL) did not cause a statistically significant AHR elevation in asthmatic mice, suggesting that AHR increase was not due to acute responses to GO administration.

GO Exposure Facilitated Airway Remodeling in Sensitized Animals. Microscopic evaluation of the lungs of mice in PBS control group reveals normal morphology of conducting and respiratory airways (Figure 3A). Lungs of mice exposed to GO (GO/S/cont group) revealed deposition of brown-pigmented particles in small airways and numerous interstitial aggregates of pigment-laden macrophages (Figure 3B, arrows). GO exposure also caused mild interstitial lymphocytic infiltration without evidence of airway remodeling. In OVA-treated asthmatic animals (Figure 3C), epithelial hypertrophy/hyperplasia, goblet cell hyperplasia, smooth muscle hypertrophy, and intense lymphohystiocytic infiltration were apparent, indicating airway remodeling (Figure 4). In mice treated with GO during the sensitization phase (GO/SENT), interstitial aggregates of GO-laden macrophages were seen (Figure 3D, arrows). Epithelial hypertrophy/hyperplasia in mice of the GO/SENT group was as noticeable as in the OVA/ALL group, and other morphologic features of airway remodeling were more prominent (Figure 4 and Table 1). Compared to the OVA/ALL group, a significant increase in the number of goblet cells (15 ± 1 *vs* 10 ± 1 per 100 μm), subepithelial fibrosis (32 ± 0.6 μm *vs* 22 ± 0.8 μm), and smooth muscle layer (24 ± 0.6 μm *vs* 15 ± 0.9 μm) was seen in OVA/SENT mice.

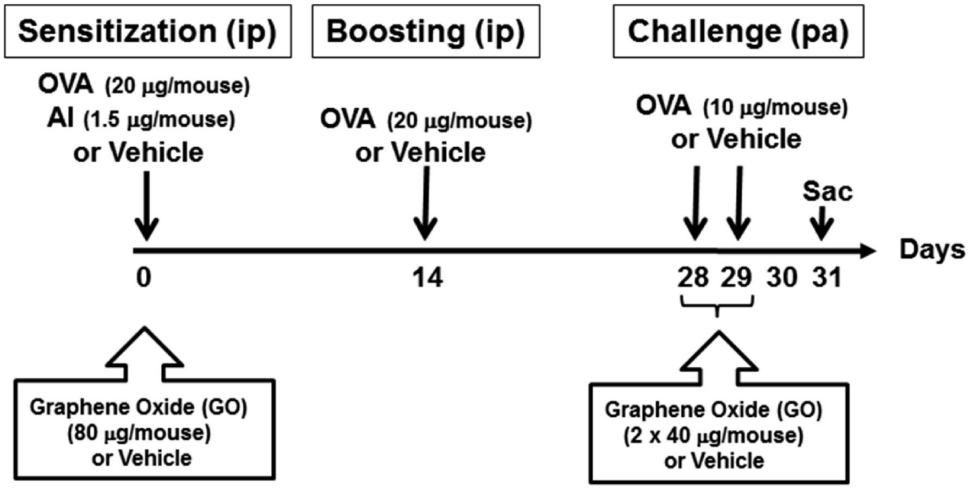

D0		D14		D28		D29		Groups
OVA	GO	OVA	GO	OVA	GO	OVA	GO	
+		+		+		+		OVA/ALL
+	+	+		+		+		GO/SENT
+		+		+	+	+	+	GO/CHAL
	+							GO/S/cont
					+		+	GO/C/cont
								PBS

Figure 1. Scheme of experimental design and details of groups exposed to GO. On day 0 of the experiment, BALB/c mice were treated with saline or GO particles *via* pharyngeal aspiration with or without OVA sensitization by intraperitoneal (ip) injection. Following this, a booster ip injection of OVA or saline was administered on day 14. On days 28 and 29, mice were further challenged with pharyngeal aspiration of either OVA or saline or treated with GO along with OVA. Mice were sacrificed on day 31, *i.e.*, 48 h after the last OVA challenge. The table summarizes in brief the details corresponding to the different treatment and exposure groups employed in this study. The treatment groups included (given at day 0; day 14; days 28−29) OVA/ALL (OVA sensitization; OVA boosting; OVA challenge), GO/SENT (OVA sensitization + GO; OVA boosting; OVA challenge); and GO/CHAL (OVA sensitization; OVA boosting; OVA challenge + GO). The control groups included animals treated with GO only (on day 0 or days 28−29, GO/S/cont and GO/C/cont, respectively) or vehicle (PBS).

Exposure to GO Reduced Eosinophil Accumulation, but Stimulated Macrophage Influx in the Lungs of Asthmatic Mice. A robust accumulation of eosinophils in BALF, as expected, accompanied OVA sensitization and challenge in OVA/ALL mice (up to $1.1 \pm 0.2 \times 10^6$ cells/mL *vs* none in PBS control). GO exposure at the time of OVA sensitization (GO/SENT group) reduced eosinophil counts compared to OVA/ALL-treated mice ($(0.5 \pm 0.1) \times 10^6$ cells/mL, $p < 0.05$). GO administration in nonsensitized animals (GO/S/cont group) did not induce eosinophil influx (Figure 5). However, GO treatment on day 28/29 (GO/C/cont group) and during OVA challenge (GO/CHAL group) facilitated transient neutrophil accumulation in BALF (Figure 5); this effect was not observed in mice exposed to GO during OVA sensitization (GO/SENT group) or on day 0 (GO/S/cont). Neutrophil counts in BAL of mice exposed to GO during OVA challenge (GO/CHAL group) were elevated up to $(0.6 \pm 0.3) \times 10^6$ *vs* $(0.2 \pm 0.1) \times 10^6$ cells/mL in OVA-only (OVA/ALL group) mice and none in PBS control animals, respectively ($p < 0.05$). Interestingly, exposure to GO during OVA sensitization (GO/SENT group) resulted in the elevation of macrophage counts in the lungs on day 31 (up to $(1.4 \pm 0.1) \times 10^6$ cells/mL in GO/SENT mice as compared to $(0.9 \pm 0.1) \times 10^6$ cells/mL in OVA/ALL animals, $p < 0.05$) (Figure 5). In GO-treated mice, BALF macrophages contained black particles, indicating the uptake/internalization of GO by macrophages (Figure 5E,F). Lymphocyte accumulation was apparent in OVA/ALL mice and GO/SENT, but not in GO/CHAL mice on day 31 after GO exposure (Figure 5). These results indicate that GO aspiration modified the inflammatory cell pattern in asthmatic animals, reducing eosinophilic inflammation in favor of the emergence of monocytes−macrophages.

GO Exposure Decreased Th2 Cytokines in BAL Fluid. To further study the pulmonary responses to GO exposure, the levels of IL-4, IL-5, IL-13, TNF-α, IL-6, IFN-γ, IL-12p70, IL-10, and IL-17 in BAL fluid of exposed animals were determined. OVA sensitization/challenge resulted in substantial elevation of Th2 cytokines in BALF (OVA/ALL group, Figure 6, $p < 0.05$). Indeed, in OVA-only treated mice, IL-4 levels peaked at 260 ± 70 pg/mL. However, in GO/SENT-treated mice the levels of IL-4 were significantly decreased and averaged at 80 ± 20 pg/mL ($p < 0.05$, Figure 6). The levels of IL-5 in BALF were also reduced in GO/SENT mice as compared to OVA-only exposed animals (Figure 6,

400 ± 60 pg/mL *vs* 270 ± 55 pg/mL, respectively, $p < 0.05$). IL-13 reached 63 ± 17 pg/mL in OVA-only exposed mice (OVA/ALL), as compared to 21 ± 6 pg/mL in GO/SENT mice or 25 ± 10 pg/mL in GO/CHAL mice ($p < 0.05$, Figure 5). Increases in IL-6 and TNF-α levels were seen only 48 h after GO administration in both OVA-sensitized and vehicle-treated animals (data not shown). The levels of IFN-γ, IL-12p70, IL-10, and IL-17 in BALF were below the detection limit of the assay. Overall, GO aspiration reduced the release of Th2 cytokines in the lungs of asthmatic mice.

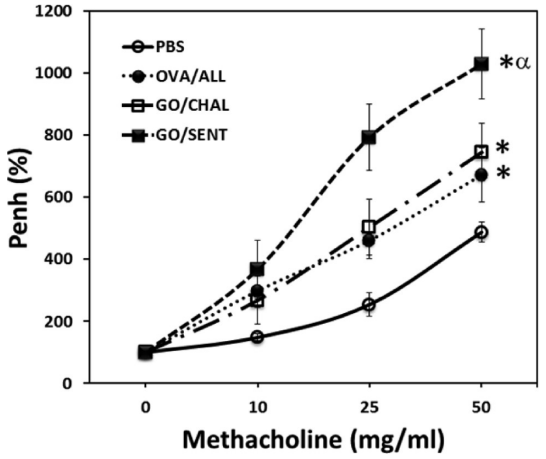

Figure 2. GO given at sensitization promotes airway hyperresponsiveness. The responsiveness of mouse airways was measured on day 31 (*i.e.*, 48 h after the last OVA challenge) using a single chamber, whole-body plethysmograph system. Mice were exposed to increasing concentrations (10, 25, 50 mg/mL) of aerosolized methacholine (MCh). The baseline was measured for 3 min prior to MCh exposure. After baseline measurements, MCh is nebulized for 1.5 min, and airway reactivity was measured (2 min/concentration). Airway reactivity was expressed as Penh (enhanced pause) values. For details corresponding to the different treatment groups please refer to Figure 1. Data are displayed as mean ± SEM for 6 mice per group, *$p < 0.05$ *vs* OVA/ALL treatment, and $^{\alpha}p < 0.05$ OVA/ALL *vs* PBS treatment.

GO Attenuated Th2 Immune Responses in Favor of Th1 Polarization. To evaluate the effects of pulmonary GO exposure on adaptive immune responses to OVA sensitization, the levels of total and OVA-specific IgE as well as OVA-specific IgG1 and IgG2a in the serum were assessed. OVA sensitization resulted in a dramatic increase in the serum levels of IgE and IgG1 (Figure 7), as compared to nonsensitized animals. Notably, GO aspiration substantially decreased both total and OVA-specific IgE levels (Figure 7, 2000 ± 230 ng/mL in GO/SENT mice *vs* 5800 ± 500 ng/mL in OVA/ALL animals, $p < 0.05$). OVA-specific IgG1, a Th2-associated antibody, was also significantly lower in GO/SENT mice as compared to OVA/ALL counterparts: 40 ± 3 U/mL *vs* 60 ± 5 U/mL, respectively ($p < 0.05$). Importantly, a Th1-associated immunoglobulin, IgG2a, was significantly elevated in GO/SENT mice compared to OVA/ALL controls: 2400 ± 730 U/mL *vs* 250 ± 12 U/mL, respectively ($p < 0.05$). Administration of GO alone or vehicle did not result in elevation of any of the measured immunoglobulins. Taken together, these results suggest that pulmonary exposure to GO altered immune responses to OVA, reducing Th2-dependent and activating Th1-dependent pathways.

GO Exposure Stimulated CHI3L1 and AMcase Accumulation in the Lungs. To test whether GO exposure altered the levels of chitinases implicated in asthma development, the content of CHI3L1 and AMCase in BALF of GO-treated mice on day 7 postexposure was detected (Figure 8). In exposed animals, the levels of BALF CHI3L1 was markedly increased and peaked at 147.3 ± 26.9 pg/mL, as compared to 7.2 ± 4.4 pg/mL in control mice ($p < 0.05$). BALF AMCase levels were 676.9 ± 310.2 ng/mL in exposed mice *vs* 21.8 ± 10.1 ng/mL in controls ($p < 0.05$). These data provide the very first

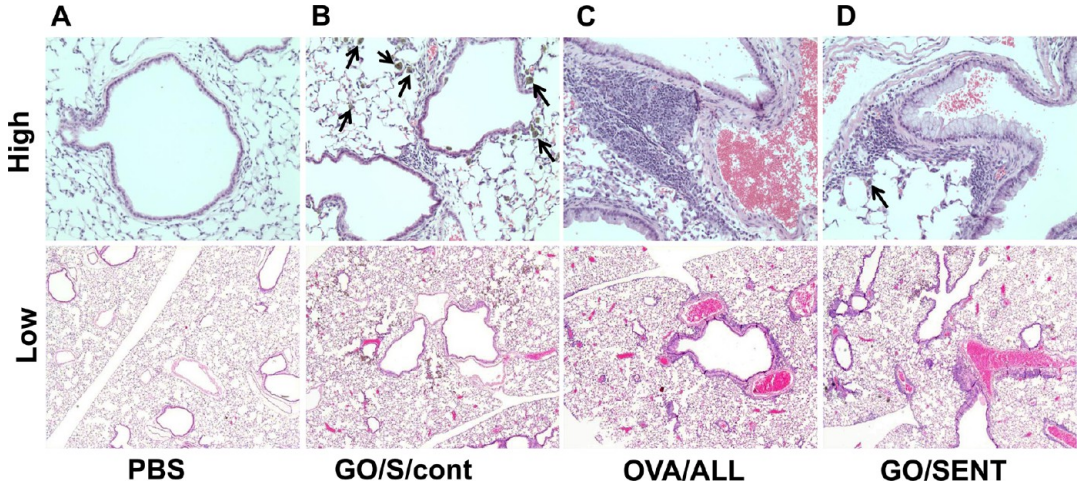

Figure 3. GO exposure promotes airway remodeling in allergen-sensitized mice. High and low power views of the light photomicrographs of representative histopathology of mouse lung tissue on day 31 postexposure to GO and/or OVA: (A) PBS; (B) OVA/ALL; (C) GO/S/cont; (D) GO/SENT exposure. The presence of interstitial pigment-laden macrophages containing GO particles is indicated by arrows.

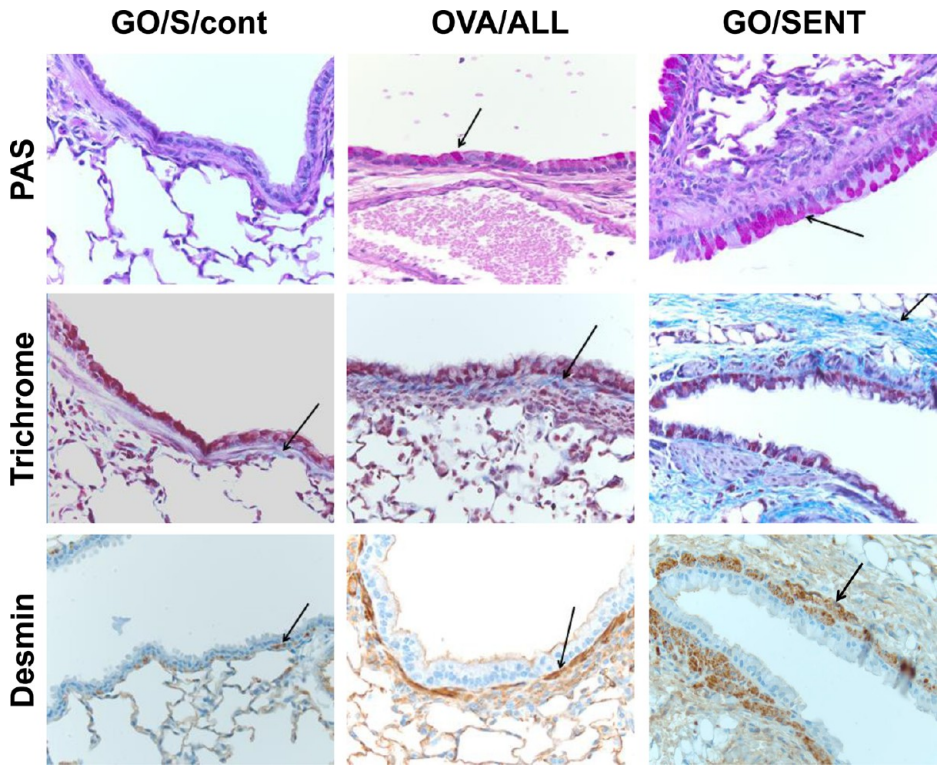

Figure 4. Pharyngeal aspiration of GO during OVA-sensitization increases epithelial fibrosis, smooth muscle hypertrophy, and goblet cell hyperplasia. Photomicrographs of representative mouse lung sections on day 31 postexposure to GO and/or OVA. Lung sections were stained with PAS/diastase to show goblet cells (in red), with trichome to show epithelial fibrosis (in blue), and with desmin to show smooth muscles (in brown). The identified morphologic alterations in each case are highlighted with arrows.

TABLE 1. Morphometric Evaluations of Airway Remodeling upon Pulmonary Exposure to GO in a Murine Model of Asthma[a]

	PBS	GO/S/cont	OVA/ALL	GO/SENT
epithelial thickness (in μm)	7.1 ± 0.8	9.1 ± 0.5	24.9 ± 0.9[b]	27.1 ± 0.9[b]
smooth muscle thickness (in μm)	6.0 ± 0.4	7.0 ± 0.5	15.0 ± 0.9[b]	24.1 ± 0.6[b,c]
subepithelial fibrosis (in μm)	3.0 ± 0.4	3.0 ± 0.5	21.9 ± 0.8[b]	32.0 ± 0.6[b,c]
goblet cells (per 100 μm)	2.0 ± 0.6	2.0 ± 0.6	10.0 ± 0.9[b]	14.6 ± 0.9[b,c]

[a] Data are shown as mean ± SEM. [b] $p < 0.05$ *vs* PBS treatment. [c] $p < 0.05$ *vs* OVA/ALL treatment.

evidence that GO could stimulate chitinase accumulation in the lungs of treated mice.

GO Induced CHI3L1 and AMcase in Alveolar Macrophages. To determine if AM could be the source of CHI3L1 and AMCase in the lungs of GO-treated mice, the production of these chitinases by isolated alveolar macrophages (AM) *ex vivo* was next assessed (Figure 8). The levels of CHI3L1 in culture supernatants of AM isolated from GO-treated animals peaked at 99.8 ± 35.7 pg/mL, as compared to 7.1 ± 3.6 pg/mL in control cells ($p <$ 0.05). AMCase levels were 632.6 ± 171.4 pg/mL in AM cultures from exposed mice *vs* undetectable levels in controls. These data showed that GO directly stimulated CHI3L1 and AMCase release by AM.

GO Interacts with AMCase and CHI3L1 in Close Proximity to the Chitin/Oligosaccharide Binding Site. To investigate if GO, similar to chitins, can directly bind/interact with chitinases AMCase and CHI3L1, we first performed molecular modeling studies to predict the interaction site of GO on chitinases. The preferred binding conformations in each case are shown in Figure 9. The GO was predicted to interact with AMCase and CHI3L1 at two different binding sites, site1 and site2. Residues that are predicted to be within 5 Å of GO at each binding site are listed in Table 2. The preferred binding site, site1, was located in close proximity to the chitin/active binding site in AMCase and the oligosaccharide binding site in CHI3L1, either completely (Figure 9A) or partially (Figure 9B) blocking the binding cavity. The predicted binding energies of GO to AMCase and CHI3L1 at site1 were −20.0 and −19.6 kcal/mol, respectively. Most importantly, the interaction of GO at site1, completely occupying the entrance of the active site cavity, overlaps with the inhibitor binding site in AMCase (Figure 9A). Especially, the predicted binding site residues W31, W99, N100, A295, and E297 (Table 2)

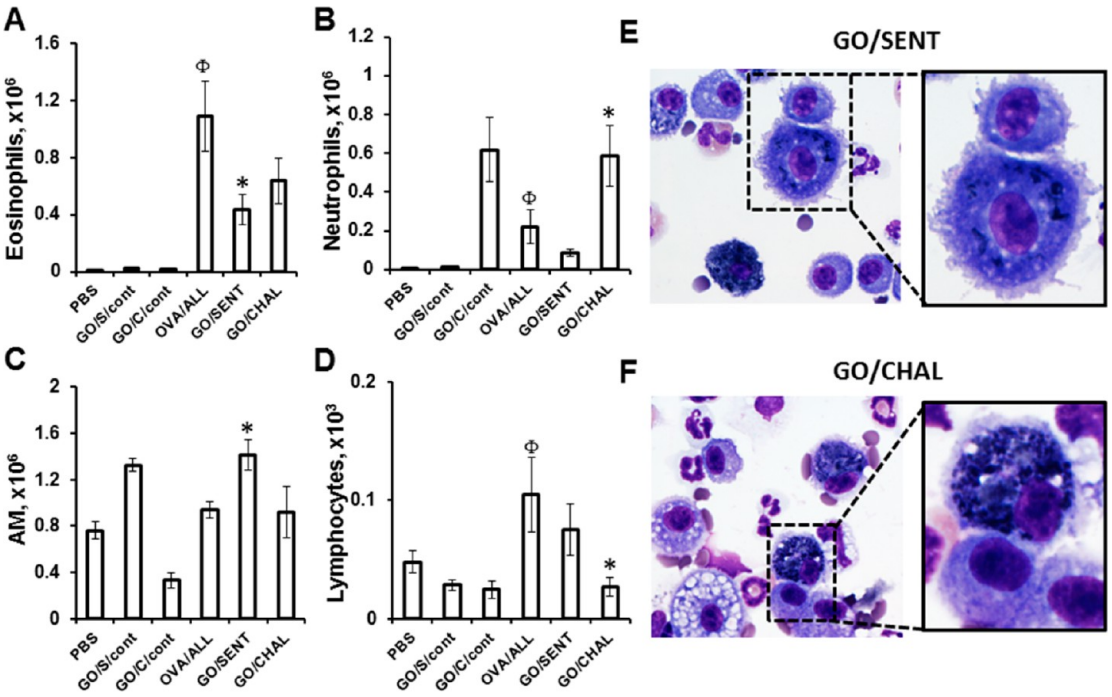

Figure 5. GO-induced pulmonary inflammatory responses. Cell profile of bronchoalveolar lavage samples from mice 48 h after the last OVA challenge (*i.e.*, on day 31 postexposure): (A) eosinophils, (B) neutrophils, (C) macrophages, (D) lymphocytes. Photomicrographs of BALF cells (cytospin preparations stained with Diff-Quik) from (E) GO/SENT and (F) GO/CHAL groups. Data are presented as mean ± SEM for 6 mice per group, *$p < 0.05$ *vs* OVA-ALL treatment ($N = 3$). $^{\Phi}p < 0.05$ OVA/ALL *vs* PBS treatment.

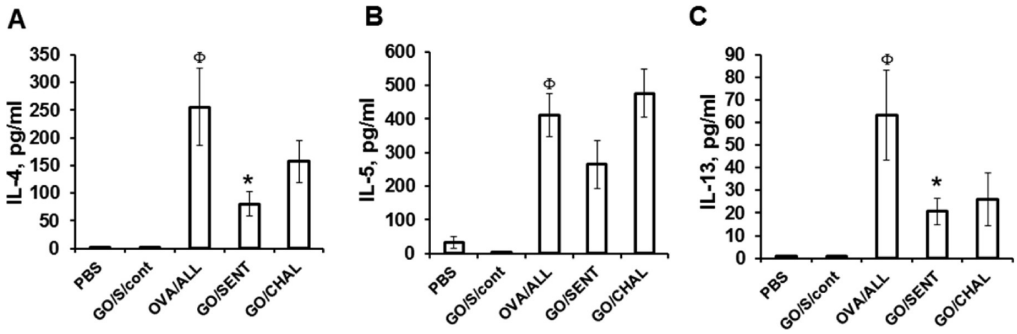

Figure 6. Pharyngeal aspiration of GO during OVA-sensitization suppresses Th2 cytokines in the BAL fluid of mice. Cytokine accumulation in bronchoalveolar lavage samples from mice 48 h after the last OVA challenge (*i.e.*, on day 31 postexposure): (A) IL-4, (B) IL-13, (C) IL-5. Levels of IFN-γ, IL-10, and IL-12p70 in BAL fluid were below the assay sensitivity. Data are shown as mean ± SEM for 6 mice per group, *$p < 0.05$ *vs* OVA/ALL treatment, and $^{\Phi}p < 0.05$ OVA/ALL *vs* PBS treatment ($N = 3$).

were shown to interact with and stabilize AMCase inhibitors bisdionin-C and -F and others.[26,27] However, this was not the case for CHI3L1 protein. GO binding to CHI3L1 at site1 results in the partial occlusion of the entrance to the cavity. Notably, the chitinase-3-like proteins such as CHI3L1 lack Chitinase activity due to mutations within the active site compared to AMCase.[21] Thus, the occlusion of the entrance to the chitin binding site by GO in AMCase—interfering with the binding/catalysis/hydrolysis of chitin polymers—could lead to the inhibition of its activity and/or signaling. Further, these results also suggest that GO interaction with chitinases, in close proximity to chitin/oligosaccharide binding site leading to immobilization of chitinases on its surface, could act as a signal of chitinase insufficiency, triggering their compensatory synthesis by macrophages.

GO Reduces the Chitinolytic Activity. To verify whether GO inhibits AMCase enzymatic activity, as predicted by molecular modeling, we measured chitinolytic activity in the BAL fluid of mice on day 31 post OVA sensitization and/or GO exposure (Figure 10A). The chitinolytic activity increased significantly in the BAL samples from mice that were OVA-sensitized and challenged (OVA/ALL). Treating these mice with GO during OVA sensitization (GO/SENT group) or OVA challenge (GO/CHAL group) significantly reduced OVA-induced AMCase enzymatic activity in the BALF by 56.2% and 8.5%, respectively (Figure 10A). However, GO administration in nonsensitized (GO/S/cont group) and nonchallenged

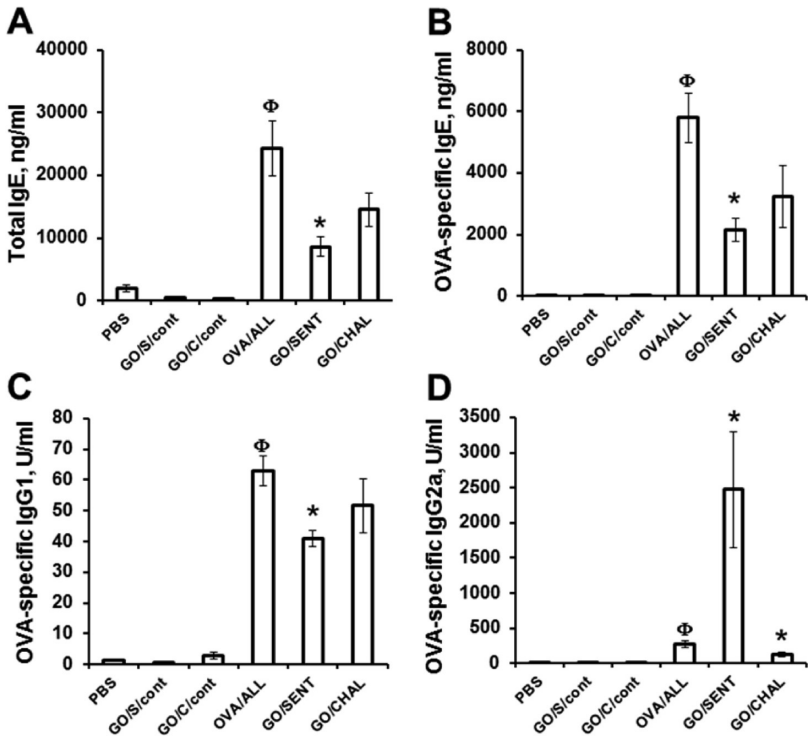

Figure 7. GO exposure attenuates Th2 immune responses in a murine model of asthma. Levels of total and OVA-specific IgE, IgG1, and IgG2a in the serum of mice 48 h after the last OVA challenge (*i.e.*, on day 31): (A) total IgE, (B) OVA-specific IgE, (C) OVA-specific IgG1, (D) OVA-specific IgG2a. Data are displayed as mean ± SEM for 6 mice per group, *$p < 0.05$ *vs* OVA/ALL treatment, and $^{\Phi}p < 0.05$ OVA/ALL *vs* PBS treatment ($N = 3$).

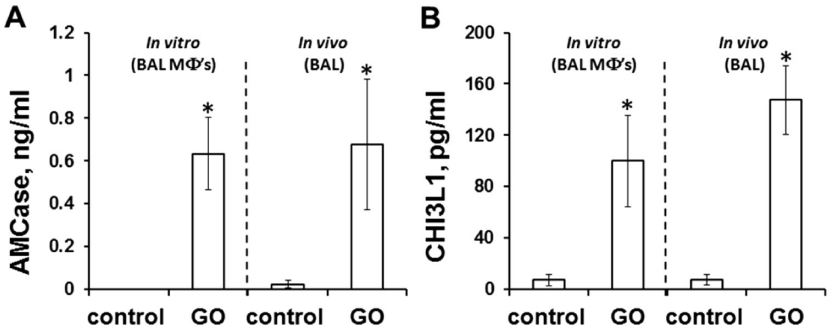

Figure 8. GO stimulates accumulation of chitinases (AMCase and CHI3L1) in the lungs of mice. Levels of chitinase 3-like 1 (CHI3L1) and acidic mammalian chitinase (AMCase) were evaluated in BAL fluid of mice 7 days after exposure to GO (A, B) or supernatants from cultured BAL macrophages: (A) AMCase; (B) CHI3L1. Alveolar macrophages were isolated from BAL fluid of mice exposed to GO or vehicle (24 h after exposure). The adherent cells (macrophages) were collected and seeded at a concentration of 2×10^5 cells/mL in 96-well plates in complete medium in the presence of recombinant mouse IL-4 (1000 U/mL). Forty-eight hours later, culture supernatants were collected and used for chitinase assay. *$p < 0.05$ *vs* PBS ($N = 2$).

(GO/CHAL group) animals did not induce any chitinolytic activity (Figure 10A). Further, to provide direct evidence for the specific inhibition of AMCase activity by GO, we evaluated the chitinolytic acivity using recombinant human AMCase (hAMCase), stably expressed in HEK-293 cells (Figure 10B). After 30 min of incubation, GO treatment resulted in a concentration-dependent inhibition of hAMCase activity with an estimated binding constant (K_D) of 326.1 ± 29.9 μg/mL. However, the inhibitory potential of GO was lower compared to a known inhibitor of AMCase, bisdionin C (Figure 10C, inset). The K_D of bisdionin C was estimated to 4.3 ± 1.2 μg/mL. Assuming that the oxygen-containing functionalities—involved in interactions with AMCase—represent only a fraction of the GO surface, our results strongly suggest that GO binds and inhibits the activity of AMCase.

DISCUSSION

Airway hyperresponsiveness, pulmonary eosinophilia, and mucus hypersecretion, along with atopic sensitization, are well-described hallmark features of asthma. Several mouse models have been developed that closely resemble the human asthmatic phenotype. The use of aluminum hydroxide adjuvant in OVA sensitization protocols followed by OVA challenge has

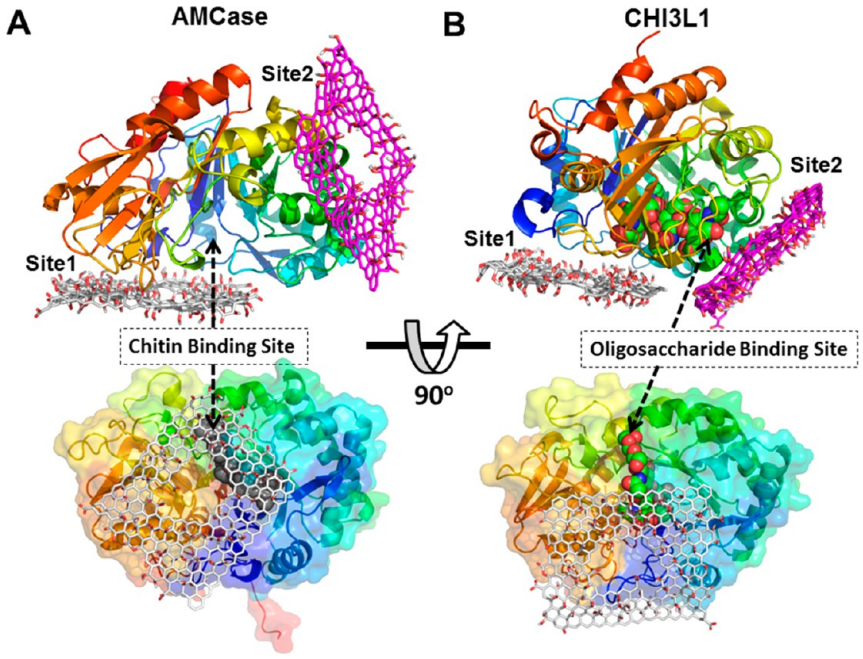

Figure 9. Molecular modeling of GO binding to AMCase and CHI3L1. The two predicted binding poses of GO, site1 and site2, in each case are represented as sticks and colored in gray and magenta, respectively: (A) AMCase; (B) CHI3L1. The structures of chitinases are represented as cartoons and colored red/blue to emphasize the N/C terminus. To highlight the active binding site cavity of chitinases, bound ligand/cavity space is represented as spheres. The oxygen and hydrogen atoms corresponding to the organic molecules—such as GO and small molecules bound to CHI3L1—are colored in red and white, accordingly.

TABLE 2. Possible Interaction Sites of Graphene Oxide (GO) on the Chitinases AMCase and CHI3L1[a]

	binding site (no. of conformations)	binding energy (in kcal/mol)	5 Å residues
AMCase	Site1 (8/9)	−20.0	W31, Y34, P36, G37, I69, E70, W99, N100, F101, G102, R145, S217, I272, S286, G287, A288, G289, P290, A291, G292, P293, A295, K296, E297, S298, N331, V332
	Site2 (1/9)	−17.8	P149, Q150, K152, H153, I188, S189, Q192, S193, G194, E196, P198, Q199, Q202, Y240, Y245, Y249, K251, D252, N253, G254
CHI3L1	Site1 (6/9)	−19.6	Q33, Y34, E36, N60, W69, E70, W71, W99, N100, F101, G102, Q104, R105, T266, S279, G280, P281, G282, F283, P284, G285, R286, K289, E290, A291, N323
	Site2 (3/9)	−19.1	R144, R145, K182, V183, D186, S187, A211, W212, R213, G214, T215, R224, E227, D228, S230, P231, D232, R233, F234, A268, G275, A276, P277, I278, S279

[a] A list of all residues (within 5 Å) that stabilize the two predicted binding sites along with the lowest binding energy and the total number of conformations (out of the top 9 conformations) observed in each case is provided.

been shown to produce a robust Th2-mediated asthma-like disease in mice.[28,29] Numerous recent studies have stipulated on the detrimental effects of pulmonary nanoparticle exposure on immune-mediated diseases. In particular, carbon nanotubes, carbon black, and diesel exhaust particles (DEP) have been reported to potentiate Th2-driven type I hypersensitivity reactions in several murine models of asthma.[10,11,30] Graphene oxide is a promising carbonaceous nanomaterial with unique physical−chemical properties suggested for various medical and industrial applications. Recent studies have shown that GO can cause acute inflammation and has the potential to induce severe and persistent lung injury in animal models.[31−33] However, the effects of pulmonary exposure to GO on immune responses and pathological outcomes in murine models of asthma have not been previously investigated.

Here we have demonstrated that pulmonary GO exposure upon initial OVA sensitization augments airway responsiveness as measured by the methacholine challenge method. As methacholine acts directly on airway smooth muscle, our data indicate that airway smooth muscle hypertrophy is more prominent in the GO/SENT group than in the OVA/ALL group (Figure 2). Airway remodeling, including subepithelial fibrosis, airway smooth muscle hypertrophy and/or hyperplasia, increased vascularity, and changes in extracellular matrix, often develops secondary to airway inflammation.[34−38] A combination of increased contractility/mass of the airway smooth muscle, increased airway wall thickness, and reduced airway caliber has been implicated in AHR.[39] In our study, histopathologic evaluation of the airways in mice exposed to GO during sensitization revealed that goblet cell hyperplasia and

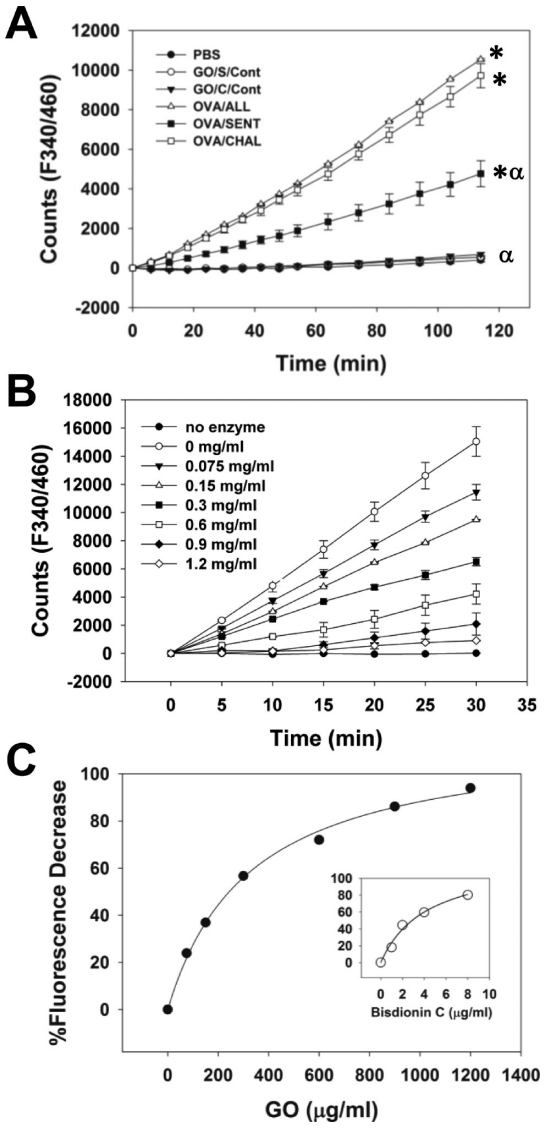

Figure 10. GO exposure inhibits the chitinolytic activity of AMCase. (A) Time course of chitinolytic activity in the BAL fluid of mice 24 h after the last OVA challenge (*i.e.*, on day 31). (B) Dose-dependent changes in the enzymatic activity of recombinant human AMCase (hAMCase) upon addition of GO. (C) Decrease in the reaction rate of the enzyme upon addition of various concentrations of GO. A dose-dependent decrease in hAMCase upon addition of a known inhibitor, bisdionin C (IC_{50}: 20 μM), is shown as an inset for comparison purposes. Data are shown as mean ± SEM, *$p < 0.05$ *vs* PBS treatment, and $p < 0.05$ *vs* OVA/ALL treatment ($N = 3$).

smooth muscle hypertrophy were more prominent compared to the OVA/ALL group (Figures 3, 4). These facts suggest that extended airway remodeling induced by GO exposure contributes to the enhanced AHR in GO-treated mice sensitized to OVA.

Surprisingly, GO exposure upon initial OVA sensitization suppressed Th2-driven responses. In particular, GO treatment reduced the levels of IL-4, IL-5, and IL-13 in BALF, as well as eosinophil accumulation in the lungs (Figures 5, 6). The Th2-derived cytokines, IL-4 and IL-13, have been widely implicated in mediating increased mucus production and early AHR, whereas IL-5 plays a pivotal role in inducing eosinophilic inflammation.[40] Moreover, the levels of OVA-specific and total IgE and OVA-specific IgG1 were also decreased in the serum of GO/SENT mice as compared to OVA/ALL animals (Figure 7). It is well known that IgE-mediated allergic responses are the most common inducers of AHR, associated with the binding of IgE antibodies to surface receptors on mast cells and eosinophils and cross-linking of receptor-bound IgE with antigens, resulting in the release of inflammatory mediators.[41]

However, our results show that elevated AHR in GO-treated mice is independent from eosinophilic airway inflammation and Th2-mediated immune response and, thus, is driven by other mechanisms. In contrast to eosinophil levels, a significant increase in the accumulation of macrophage population was seen upon GO exposure in the lungs (Figure 5). Several studies have shown that activated macrophages can produce large amounts of chitinase and chitinase-like molecules.[42−44] We found that GO exposure substantially increased the levels of both AMCase and CHI3L1 in BALF (Figure 8). A significant contribution of mammalian chitinases and chitinase-like proteins (CLP) to airway remodeling and hyperresponsiveness was reported recently.[45] Considering this, we hypothesized that direct stimulation of macrophages by GO could induce AMCase and CHI3L1 production by these cells, contributing to extended airway remodeling and AHR. We tested this by evaluating the levels of AMCase and CHI3L1 produced by macrophages isolated from BALF of animals exposed to GO. Indeed, GO stimulated the production of the chitinases AMCase and CHI3L1 by macrophages (Figure 8). Chitinases, belonging to the 18 glycosyl hydrolase family, are expressed in a wide range of organisms from prokaryotes to eukaryotes, including mammals. Chitinases are hydrolytic enzymes that break down glycosidic bonds in chitin, a major component of the insect exoskeletons and fungal cell walls. In murine allergic models, chitin administration has been reported to alleviate allergic responses. Administration of chitin increased alveolar macrophages, decreased lung eosinophils, and reduced IgE levels in the serum. The responses triggered by GO during OVA sensitization in this study were strikingly similar to those induced by chitin. Importantly, chitin molecules modulate innate immune responses by binding to receptors on cells that specifically recognize pathogen-associated molecular patterns (PAMPs).[46,47] Macrophages were shown to be stimulated by chitin molecules both *in vitro* and *in vivo via* Toll-like receptor (TLR)-dependent mechanisms.[48,49] Recent studies have suggested the role of TLRs for GO-induced effects on macrophages and their uptake by cells.[50,51] On the basis of the similarities in responses to chitin and GO exposure, we speculate that macrophages recognize GO as a PAMP, which, similar to

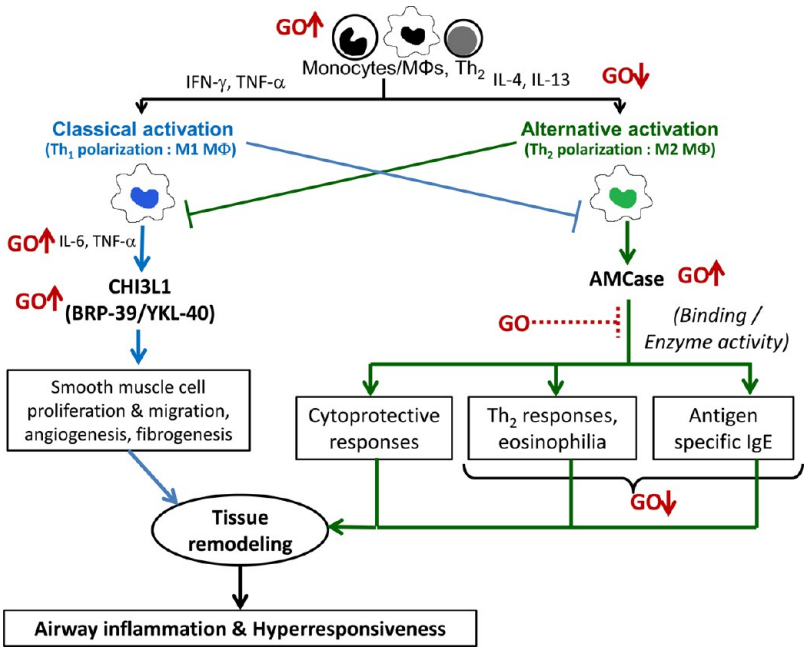

Figure 11. Scheme highlighting potential mechanisms of GO-induced airway remodeling and AHR in a murine model of asthma. Depending on the type of inflammatory cytokines available, macrophages can be activated *via* a classical (Th1: TNF-α, IFNγ) or alternative (Th2: IL-4, IL-13) mechanism. Classically activated macrophages (M1) exhibit a Th1-like phenotype and elicit chronic inflammation and tissue injury responses. Alternatively activated macrophages (M2), on the other hand, display a Th2-like phenotype and tend to resolve inflammation and promote wound healing by facilitating anti-inflammatory, antiapoptotic, and fibrogenic responses. Alternatively activated macrophages may play a major role in several pathologies, including allergy and asthma.

chitin, may be engulfed and phagocytozed. The presence of particle-laden macrophages in the lung and BALF (Figures 3, 5E,F) and the predicted interaction sites of GO in close proximity to the chitin/oligosaccharide binding site on chitinases further support this notion (Figure 9).

AMCase has been reported to play a critical role in airway inflammatory responses and remodeling in chitin-free conditions, with its expression majorly driven by Th2 cytokines IL-4 and IL-13.[52] Despite substantial increase in AMCase levels upon GO exposure (Figure 8), a decrease in eosinophilia in BAL fluid, Th2 inflammation, and serum total IgE was found in mice treated with GO during sensitization (Figures 5−7). Inhibition of the enzymatic/chitinase activity of AMCase has been previously reported to significantly alleviate features of allergic inflammation, including eosinophilia.[27,52,53] It was shown that chitinase inhibitors significantly ameliorated Th2 inflammation and airway hypersensitivity, in part by inhibiting IL-13 pathway activation, whereas IL-13 caused induction of AMCase by epithelial cells and macrophages underlying the airway hyperresponsivenes and inflammatory cell infiltration after exposure to an allergen in murine models of asthma.[27,52,53] While our data demonstrated the GO-induced increase of the expression of AMCase in the lung, the enzymatic chitinolytic activity was reduced (Figure 10). The potential for the enzyme inhibition by GO was further supported by previous studies, where GO was found to inhibit the activity of alpha-chymotrypsin.[54] This is further corroborated by our molecular modeling studies, where GO was predicted to preferentially bind at the entrance of the catalytic site of AMCase, mimicking interactions with AMCase inhibitors.[26,27] Such interaction of GO with AMCase, significantly occupying/occluding the opening of the active site (Figure 9A), may interfere with the role of AMCase in allergic inflammation and asthma. It is possible that GO affects both the enzyme activity dependent and independent mechanisms of AMCase. Under this assumption, GO can down-regulate allergen-induced IgE production and lung inflammation, including eosinophilia in OVA-sensitized mice by interfering with the enzymatic activity and/or signaling mechanisms of AMCase (Figure 11). Future studies involving the use of transgenic mice deficient in AMCase or CHI3L1 are warranted to establish a direct link between GO exposure, chitinase stimulation/inhibition, and augmented airway modeling.

YKL-40, the human homologue of CHI3L1, has been associated with airway remodeling, hyperresponsiveness, and decreased lung function.[55] It can directly increase bronchial smooth muscle cell proliferation and migration through PAR-2-, AKT-, ERK-, and p38-dependent mechanisms.[56] In our study, the expression of CHI3L1 in the lung was significantly increased by GO exposure. At the same time, the degree of airway remodeling and increased airway hyperresponsiveness were more prominent in the GO/SENT group as compared to OVA/ALL mice and thus may point

toward a CHI3L1-dependent mechanism. Interestingly, Homer *et al*. reported in two different models of Th2 inflammation that Ym1 and AMCase are exclusively expressed in proximal and distal airway epithelium, respectively.[57] Differential effects of GO on tested chitinases *in vitro* (Figures 9, 10) and differential penetration of GO in the lung tissue may explain the unexpected bidirectorial effects of GO on Th2 responses, macrophage and eosinophil homing, and tissue remodeling in our model of GO modulation of asthma development. These results may have an important clinical implication, since it was recently shown that pediatric patients with severe, therapy-resistant asthma have higher levels of YKL-40 than do healthy controls and that YKL-40 might serve as a biomarker of asthma severity and airway remodeling in children.[58]

Interestingly, OVA-specific IgG2a, a Th1-associated antibody, was also substantially elevated exclusively in GO/SENT mice, providing additional evidence of GO-induced suppression of Th2-mediated immune response in favor of Th1 polarization (Figure 11). However, this was the case neither in GO-vehicle nor in GO/CHAL mice (Figure 5). This clearly indicates that the presence of GO or factors such as chitinases that are released upon GO stimulation during an allergen sensitization triggers such responses. This notion is further supported by previous immunization studies in mice.[59,60] Immunizations using chitinases in the presence of adjuvants such as aluminum, as used in this study, elicited strong IgG responses including IgG2a.[59,60] The use of chitosan-based adjuvants during vaccination also induced significantly enhanced levels of IgG1 and IgG2a in the serum.[46] Further, mice immunized with Derf2-47-67-loaded chitosan particles had increased levels of Der f-specific IgG2a in the serum.[61] Thus, it is tempting to speculate that the induction of chitinases by macrophages upon GO exposure together with aluminum adjuvant or GO acting as an adjuvant by itself during allergen sensitization leads to the induction of IgG2a expression. However, GO-induced suppression of Th2 responses in favor of Th1 responses allowing isotype switching in activated B cells cannot be discounted (see Figure 11 for a schematic summary).

Collectively, our results indicated that GO-induced immune responses down-regulated Th2-facilitated IgE production and lung eosinophilia in a mouse model of asthma, proposing a novel mechanism of nanoparticle-induced airway remodeling and AHR in asthma (Figure 11). To this point, we demonstrated that GO was able to modulate allergic immune response in a murine model of OVA-induced asthma. We showed that GO augmented AHR independently from eosinophil accumulation and IgE production. We proposed that direct stimulation of mammalian chitinases in macrophages by GO could be a new mechanism underlying GO-induced airway remodeling (Figure 11). Further investigations, perhaps with a deeper focus on understanding the relation between augmented airway remodeling and stimulation/activity/signaling mechanisms of chitinases, are required to fully explore the mechanisms of immune response modulation induced by GO exposure. Our findings emphasize the importance of carefully assessing the immunomodulatory effects of nanoparticles considered for industrial and biomedical applications; conversely, if appropriately controlled, such properties may also be exploited for therapeutic gain similar to chitosan-based adjuvants in vaccines.

CONCLUSIONS

Pulmonary exposure to graphene oxide suppressed Th2-mediated immune response and allergic inflammation in a murine model of asthma. GO aspiration augmented airway hyperresponsiveness independently from eosinophil accumulation and IgE production in asthmatic mice. Extended airway remodeling in GO-treated animals could underlie augmented AHR and could be partially attributed to the direct GO-driven stimulation of production of chitinases by alveolar macrophages. Further investigations are required to elucidate the detailed mechanisms of nanoparticle (GO)-driven modulation of Th2 immune responses in asthma.

METHODS

Particles. Graphene oxide was synthesized and characterized as described elsewhere.[62] The zeta potential of GO was −32.4. The average particle thickness was 0.61 nm, while the length and width varied from 20 nm to ∼5 μm. Stock suspensions (1 mg/mL) were prepared before each experiment in PBS, and the pH was adjusted to 7.0; suspensions were sonicated for 5 min with a probe sonicator (VibraCell, Sonics and Materials Inc., Newtown, CT, USA) and sterilized by autoclaving. Stock suspensions were diluted to achieve required concentrations and sonicated (three 1 min cycles) before use. Endotoxin content in GO suspensions was evaluated using Limulus amebocyte lysate chromogenic end point assay kit (Hycult Biotech, Inc., Plymouth Meeting, PA, USA) according to the manufacturer's instructions and found to be below the detection limit (0.01 EU/mL).

Animals. Specific-pathogen-free adult female BALB/c mice (7−8 weeks old) were supplied by Jackson Laboratories (Bar Harbor, ME, USA). Animals were individually housed in the National Institute for Occupational Safety and Health (NIOSH) facilities approved by Association for Assessment and Accreditation of Laboratory Animal Care International (AAALAC). Mice were acclimated for at least 1 week. Sterile Sani-Chip bedding (Harlan Teklad, Madison, WI, USA) was changed weekly. Animals were supplied with water and food (Harlan Teklad, 7913, NIH-31 modified mouse/rat diet, irradiated) *ad libitum* and housed under controlled light, temperature, and humidity conditions. All experiments were conducted under a protocol approved by the Animal Care and Use Committee of NIOSH (protocol

#10-AS-M-009). Six animals per study group were utilized for all *in vivo* assays, and all experiments were repeated at least two times.

As female mice of any strain are generally less aggressive toward each other and are less apt to fight than the male mice, they were preferred for studying GO treatment during OVA sensitization and/or challenge. While it is known that hormonal influences in females might interfere with toxicity studies, it is generally accepted that mice from the same lot may be used when large toxicology studies are employed for comparing different treatments/exposures. Thus, any hormonal effects would also be accounted for in the PBS control and OVA/ALL group; so any effects observed would be due to GO exposure.

Sensitization, Challenge, and GO Exposures. On day 0 of an experiment, mice were sensitized to chicken egg ovalbumin (Hyglos GmbH, Germany) by intraperitoneal injection of a sterile suspension containing OVA (20 μg/mouse) and aluminum hydroxide (Al) adjuvant (1.5 μg/mouse, Sigma, St. Louis, MO, USA) in 100 μL of PBS (Figure 1). Additionally, a group of mice were exposed to GO or vehicle by pharyngeal aspiration on day 0: a suspension of GO (80 μg/mouse in divalent ion-free PBS) or PBS was placed posterior in the throat, and the tongue was held until the suspension was aspirated into the lungs. Booster injection of OVA (ip, 20 μg/mouse) or vehicle was administered on day 14. On days 28 and 29, groups were challenged with pharyngeal aspiration of OVA (10 μg/mouse/day) in PBS or treated with GO along with OVA (40 μg/mouse/day, 80 μg cumulative dose). Experimental groups are listed as follows (Figure 1): treatment group name (treatment at day 0; day 14; days 28−29): OVA/ALL (OVA sensitization; OVA boosting; OVA challenge), GO/SENT (OVA sensitization + GO; OVA boosting; OVA challenge); GO/CHAL (OVA sensitization; OVA boosting; OVA challenge + GO). Control groups included animals treated with GO only (on day 0 or days 28−29, GO/s/cont and GO/C/cont, respectively) or vehicle (PBS). Two days (48 h) after the last OVA challenge (day 31), mice were sacrificed or used for airway hyperresponsiveness evaluation. Additional groups of animals were used for chitinase measurements and were exposed to GO only as described above.

Airway Hyperresponsiveness Evaluation. The responsiveness of mouse airways was measured on day 31 using a noninvasive whole-body plethysmograph (WBP) system (Buxco Systems Inc., Troy, NY, USA). Briefly, mice were placed in WBP of approximately 300 mL in which the animals were unrestrained and exposed to increasing concentrations (10, 25, 50 mg/mL) of aerosolized methacholine (MCh; Sigma-Aldrich). A bias flow of HEPA filtered room air of 1 LPM was drawn through each WBP. After acclimatization, the baseline was measured for 5 min prior to MCh exposure. After the baseline measurements, MCh is nebulized for 1.5 min, and pressure changes within the chamber due to respiration were monitored and recorded (2 min/concentration). The pressure signals were postprocessed using Matlab (Mathworks, Inc.) to calculate airway reactivity and expressed as enhanced pause (Penh) values. Penh is a reasonable analogue of airway responsiveness to a nonspecific inhaled stimulus, such as MCh, which provides an accepted measure for comparison between the experimental groups.

Lung Histopathology and Morphometric Analysis. Lung tissues were harvested on day 31 of the study and inflation fixed *in situ* with 4% paraformaldehyde at 10 cm H_2O for 10 min with the chest cavity open. Paraffin-embedded tissue was cut at a thickness of 5 μm, stained with hematoxylin and eosin (H&E), and examined microscopically. Sample identification was coded to ensure unbiased evaluation. Additionally, a set of lung tissue sections with a constant thickness of 5 μm was stained using PAS/diastase to highlight mucus-secreting goblet cells, by trichrome blue to highlight peribronchial fibrous tissue, and by desmin immunostain (Ventana Medical Systems, Inc.) to highlight the peribronchial smooth muscle. Unbiased morphometric analysis was performed on these stained lung tissue sections according to the principles and guidelines of basic methodological standards in lung morphometry.[63] The thickness of respiratory epithelium, subepithelial smooth muscle layer, and subepithelial fibrous layer was measured using a calibrated micrometric analyzer (Spot Insight software 5.1). At least 10 randomly chosen regions on each slide were analyzed for estimating different morphological features including number of goblet cells, thickness of smooth muscle, and fibrosis in each case. A standard area measuring 16 400 μm^2 was used for the enumeration of goblet cells. For standardization, the number of mucus-secreting goblet cells in respiratory epithelium was calculated as number of cells per 100 μm using the following formula: total number of goblet cells/total airway circumference $\times$ 100.[64] These evaluations were carried out by a single board-certified pathologist (DWG) familiar with the guidelines and standards of toxicologic pathology criteria and nomenclature for mouse lungs.[63,65−67] All morphometric measurements were performed in an unbiased (*i.e.*, blinded) fashion, where the identities of the various groups were masked and were not known by the reading pathologist.

Bronchoalveolar Lavage and Cell Counting. Twenty-four hours after the last OVA challenge (day 31), mice were sacrificed by intraperitoneal injection of sodium pentobarbital and exsanguinated. The trachea was cannulated with a blunted 22-gauge needle, and bronchoalveolar lavage was performed with cold sterile Ca^{2+}/Mg^{2+}-free PBS at a volume of 0.7 mL for the first lavage (kept separate) and 0.8 mL for subsequent lavages. A total of 5 mL of bronchoalveolar lavage fluid per mouse was collected and pooled in sterile centrifuge tubes. Pooled BAL cells were washed in Ca^{2+}/Mg^{2+}-free PBS by alternate centrifugation (200*g*, 10 min, 4 °C). Cell-free first-fraction BALF aliquots were frozen and stored at −80 °C until processed.

The degree of pulmonary inflammatory response was estimated by the total cell counts, as well as macrophages, neutrophils, eosinophils, and lymphocytes recruited into the mouse lungs and recovered from the BALF. Alveolar macrophages, neutrophils, eosinophils, and lymphocytes were identified in cytospin preparations stained with a Hema-3 kit (Fisher Scientific, Pittsburgh, PA, USA) by characteristic cell morphology, and differential counts of BAL cells were performed. Three hundred cells per slide were counted.

BAL Cytokine Analysis. Levels of cytokines were assayed in the acellular BAL fluid. The concentrations of TNF-α, IFN-g, IL-12p70, IL-10, IL-4, IL-5, IL-13, and IL-17 (sensitivity of assays is 5−7.3 pg/mL) were determined using the BD cytometric bead array, mouse Inflammation kit (BD Biosciences, San Diego, CA, USA).

Evaluation of Serum Immunoglobulins. Levels of total IgE, as well as OVA-specific IgE, IgG2a, and IgG1a, were determined in mouse serum (day 31) using commercially available ELISA kits (Alpha Diagnostic Intl. Inc., San Antonio, TX, USA) according to the manufacturer's instructions. Detection of OVA-specific immunoglobulins was used for additional identification of Th1- or Th2-inducing effects of GO.

Alveolar Macrophage Isolation and Culture. BAL cell pellets were washed three times with PBS and suspended with RPMI-1640 containing 10% heat-inactivated fetal bovine serum, 2 mM L-glutamine, 200 U/mL penicillin, and 200 mg/mL streptomycin (Invitrogen). The cell suspension was cultured overnight in 25 cm^2 flasks at 37 °C in a 5% CO_2 humidified milieu to permit the adherence of AMs. Then the nonadherent cells were removed by three washes with 2% RPMI-1640. The purity of adherent AMs was identified to be greater than 95% by morphology. The adherent cells were collected and seeded in 96-well plates (1.8×10^6 cells/plate). Forty-eight hours later, culture supernatants were collected and frozen at −80 °C for chitinase assay.

Chitinase Assays. The levels of chitinase 3-like protein 1 and acidic mammalian chitinase (AMCase or CHIA) were evaluated in BAL fluid of mice (7 days after exposure) and macrophage culture supernatants using commercially available ELISA kits. Mouse CHI3L1 ELISA assay (R&D Systems) was performed according to the manufacturer's instructions. In brief, samples, control, and standards (4000 pg/mL) were added to a microplate precoated with a polyclonal antibody specific for mouse CHI3L1. Unbound substances were washed away, and an enzyme-linked polyclonal antibody specific for mouse CHI3L1 was added, followed by a wash to remove unbound antibody−enzyme reagents. The AMCase ELISA kit was purchased from Cusabio Biotech Co. Ltd. (China, http://www.cusabio.com/). The assay was performed according to the manufacturer's

instructions. In brief, samples and standards (20 ng/mL) were added to a microplate precoated with an antibody specific for mouse CHIA. Unbound substances were removed by washing, followed by the addition of biotin-conjugated antibody specific for CHIA and subsequent washing. Horseradish peroxidase was added, and any unbound avidin−enzyme reagents were washed away. For color development in both assays, substrate solution was added, and the optical density readings at 450−540 nm were proportional to the amount of initially bound CHI3L1/CHIA.

Molecular Modeling Studies. The three-dimensional structure of GO was docked to the crystal structure of AMCase (pdbid: 3FXY:A) and CHI3L1 (pdbid: 1HJV:A) using AutoDock Vina[68] available at http://vina.scripps.edu. While the presence of rotatable bonds on the GO ligand structure imparted flexibility, structures of chitinases were considered to be rigid for docking. The grid box was centered at coordinates 23.994, −28.478, −35.646 with 80 Å units in the *x*, *y*, and *z* directions for AMCase and at 24.202, 39.202, 34.858 with 80 Å units in the *x*, *y*, and *z* directions for CHI3L1. This grid box covered the entire structure of each chitinase, making the docking unbiased for different binding sites. The resulting orientations in each case were clustered based on the position of binding on the receptor structure. The best ligand-bound chitinase receptor structure in each case was chosen based on lowest energy as well as the total number of conformations in that binding site.

Chitinolytic Activity of AMCase. The activity of AMCase was measured fluorimetrically on the basis of enzymatic hydrolysis of the 4-methylumbelliferyl-β-D-*N*,*N*′,*N*″-triacetylchitotriose (4-MU-chitotrioside, a substrate for endochitinase) with production of 4-methylumbelliferone (4-MU) using CycLex acidic mammalian chitinase fluorometric assay kit (MBL International, Woburn, MA, USA). A 10 μL volume of BAL samples (after 200-fold dilution) was used for the enzymatic assay. Fluorescence was measured at an excitation of 340 nm and emission of 460 nm for 120 min with 5−10 min intervals at 30 °C. The activity of AMCase in different samples was estimated by dividing the relative fluorescence *vs* reaction time (min). The inhibitory effects of a known chitinase inhibitor, bisdionin C (IC_{50}: 20 μM), and GO were investigated using recombinant human AMCase. Briefly, 10 μL of purified hAMCase (0.3 ng/μL) and 10 μL of 0.2 mM 4-MU-chitotrioside were added to 80 μL of chitinase assay buffer containing various concentrations of GO (0−1.2 mg/mL) or bisdionin C (0−8 μg/mL or 0−20 μM). The results of the inhibition assays are reported as percent decrease in activity (ratio of hAMCase activity in the presence and absence of inhibitor). All samples were assayed in triplicates. The binding constants of GO and bisdionon C to AMCase were estimated by fitting the percent decrease in relative fluorescence using nonlinear regression.

Statistical Analysis. Values are presented as mean values ± SEM. The significance of treatment-related differences was evaluated using either two-tailed Student's *t* test or a nonparametric Kruskal−Wallis ANOVA on Ranks followed by the Holm−Sidak test. *p* values of less than 0.05 were considered to be statistically significant.

Disclosure: The findings and conclusions in this report are those of the author(s) and do not necessarily represent the views of the National Institute for Occupational Safety and Health.

Conflict of Interest: The authors declare no competing financial interest.

Acknowledgment. This work was supported by NIOSH OH008282, NORA 0HELD015, EC-FP-7-NANOSOLUTIONS, and NIEHS R01ES019304. The authors are grateful to M. Farcas, M. Hatfield, S. Stanley, A. Cumpston, J. Cumpston, and D. Schwegler-Berry for the technical assistance.

REFERENCES AND NOTES

1. Tkach, A. V.; Shurin, G. V.; Shurin, M. R.; Kisin, E. R.; Murray, A. R.; Young, S. H.; Star, A.; Fadeel, B.; Kagan, V. E.; Shvedova, A. A. Direct Effects of Carbon Nanotubes on Dendritic Cells Induce Immune Suppression upon Pulmonary Exposure. *ACS Nano* **2011**, *5*, 5755–5762.
2. Shvedova, A. A.; Kagan, V. E.; Fadeel, B. Close Encounters of the Small Kind: Adverse Effects of Man-Made Materials Interfacing with the Nano-Cosmos of Biological Systems. *Annu. Rev. Pharmacol. Toxicol.* **2010**, *50*, 63–88.
3. Mitchell, L. A.; Lauer, F. T.; Burchiel, S. W.; McDonald, J. D. Mechanisms for How Inhaled Multiwalled Carbon Nanotubes Suppress Systemic Immune Function in Mice. *Nat. Nanotechnol.* **2009**, *4*, 451–456.
4. Foster, P. S.; Hogan, S. P.; Ramsay, A. J.; Matthaei, K. I.; Young, I. G. Interleukin 5 Deficiency Abolishes Eosinophilia, Airways Hyperreactivity, and Lung Damage in a Mouse Asthma Model. *J. Exp. Med.* **1996**, *183*, 195–201.
5. Drazen, J. M.; Arm, J. P.; Austen, K. F. Sorting out the Cytokines of Asthma. *J. Exp. Med.* **1996**, *183*, 1–5.
6. Gleich, G. J.; Kita, H. Bronchial Asthma: Lessons from Murine Models. *Proc. Natl. Acad. Sci. U.S.A.* **1997**, *94*, 2101–2102.
7. Deo, S. S.; Mistry, K. J.; Kakade, A. M.; Niphadkar, P. V. Role Played by Th2 Type Cytokines in IgE Mediated Allergy and Asthma. *Lung India* **2010**, *27*, 66–71.
8. Ngoc, P. L.; Gold, D. R.; Tzianabos, A. O.; Weiss, S. T.; Celedon, J. C. Cytokines, Allergy, and Asthma. *Curr. Opin Allergy Clin. Immunol.* **2005**, *5*, 161–166.
9. de Haar, C.; Hassing, I.; Bol, M.; Bleumink, R.; Pieters, R. Ultrafine Carbon Black Particles Cause Early Airway Inflammation and Have Adjuvant Activity in a Mouse Allergic Airway Disease Model. *Toxicol. Sci.* **2005**, *87*, 409–418.
10. Nygaard, U. C.; Hansen, J. S.; Samuelsen, M.; Alberg, T.; Marioara, C. D.; Lovik, M. Single-Walled and Multi-Walled Carbon Nanotubes Promote Allergic Immune Responses in Mice. *Toxicol. Sci.* **2009**, *109*, 113–123.
11. Inoue, K.; Yanagisawa, R.; Koike, E.; Nishikawa, M.; Takano, H. Repeated Pulmonary Exposure to Single-Walled Carbon Nanotubes Exacerbates Allergic Inflammation of the Airway: Possible Role of Oxidative Stress. *Free Radical Biol. Med.* **2010**, *48*, 924–934.
12. de Haar, C.; Hassing, I.; Bol, M.; Bleumink, R.; Pieters, R. Ultrafine but Not Fine Particulate Matter Causes Airway Inflammation and Allergic Airway Sensitization to Co-Administered Antigen in Mice. *Clin. Exp. Allergy* **2006**, *36*, 1469–1479.
13. Yang, D.; Zhao, Y.; Guo, H.; Li, Y.; Tewary, P.; Xing, G.; Hou, W.; Oppenheim, J. J.; Zhang, N. [Gd@C(82)(Oh)(22)](N) Nanoparticles Induce Dendritic Cell Maturation and Activate Th1 Immune Responses. *ACS Nano* **2010**, *4*, 1178–1186.
14. Mitchell, L. A.; Gao, J.; Wal, R. V.; Gigliotti, A.; Burchiel, S. W.; McDonald, J. D. Pulmonary and Systemic Immune Response to Inhaled Multiwalled Carbon Nanotubes. *Toxicol. Sci.* **2007**, *100*, 203–214.
15. Layachi, S.; Rogerieux, F.; Robidel, F.; Lacroix, G.; Bayat, S. Effect of Combined Nitrogen Dioxide and Carbon Nanoparticle Exposure on Lung Function during Ovalbumin Sensitization in Brown Norway Rat. *PLoS One* **2012**, *7*, e45687.
16. Granum, B.; Lovik, M. The Effect of Particles on Allergic Immune Responses. *Toxicol. Sci.* **2002**, *65*, 7–17.
17. Shvedova, A. A.; Pietroiusti, A.; Fadeel, B.; Kagan, V. E. Mechanisms of Carbon Nanotube-Induced Toxicity: Focus on Oxidative Stress. *Toxicol. Appl. Pharmacol.* **2012**, *261*, 121–133.
18. Bhattacharya, K.; Andón, F. T.; El-Sayed, R.; Fadeel, B. Mechanisms of Carbon Nanotube-Induced Toxicity: Focus on Pulmonary Inflammation. *Adv. Drug Delivery Rev.* **2013**, *65*, 2087–2097.
19. Shuhui, L.; Mok, Y. K.; Wong, W. S. Role of Mammalian Chitinases in Asthma. *Int. Arch. Allergy Immunol.* **2009**, *149*, 369–377.
20. Van Dyken, S. J.; Garcia, D.; Porter, P.; Huang, X.; Quinlan, P. J.; Blanc, P. D.; Corry, D. B.; Locksley, R. M. Fungal Chitin from Asthma-Associated Home Environments Induces Eosinophilic Lung Infiltration. *J. Immunol.* **2011**, *187*, 2261–2267.

21. Eurich, K.; Segawa, M.; Toei-Shimizu, S.; Mizoguchi, E. Potential Role of Chitinase 3-Like-1 in Inflammation-Associated Carcinogenic Changes of Epithelial Cells. *World J. Gastroenterol.* **2009**, *15*, 5249–5259.
22. Chupp, G. L.; Lee, C. G.; Jarjour, N.; Shim, Y. M.; Holm, C. T.; He, S.; Dziura, J. D.; Reed, J.; Coyle, A. J.; Kiener, P.; *et al*. A Chitinase-Like Protein in the Lung and Circulation of Patients with Severe Asthma. *New Engl. J. Med.* **2007**, *357*, 2016–2027.
23. Ober, C.; Tan, Z.; Sun, Y.; Possick, J. D.; Pan, L.; Nicolae, R.; Radford, S.; Parry, R. R.; Heinzmann, A.; Deichmann, K. A.; *et al*. Effect of Variation in Chi3l1 on Serum YKL-40 Level, Risk of Asthma, and Lung Function. *New Engl. J. Med.* **2008**, *358*, 1682–1691.
24. Brinchmann, B. C.; Bayat, M.; Brogger, T.; Muttuvelu, D. V.; Tjonneland, A.; Sigsgaard, T. A Possible Role of Chitin in the Pathogenesis of Asthma and Allergy. *Ann. Agric. Environ. Med.* **2011**, *18*, 7–12.
25. Duru, S.; Yuceege, M.; Ardic, S. Chitinases and Lung Diseases. *Tuberk Toraks* **2013**, *61*, 71–75.
26. Cole, D. C.; Olland, A. M.; Jacob, J.; Brooks, J.; Bursavich, M. G.; Czerwinski, R.; DeClereq, C.; Johnson, M.; Joseph-McCarthy, D.; Ellingboe, J. W.; *et al*. Identification and Characterization of Acidic Mammalian Chitinase Inhibitors. *J. Med. Chem.* **2010**, *53*, 6122–6128.
27. Sutherland, T. E.; Andersen, O. A.; Betou, M.; Eggleston, I. M.; Maizels, R. M.; van Aalten, D.; Allen, J. E. Analyzing Airway Inflammation with Chemical Biology: Dissection of Acidic Mammalian Chitinase Function with a Selective Drug-Like Inhibitor. *Chem. Biol.* **2011**, *18*, 569–579.
28. Shin, Y. S.; Takeda, K.; Gelfand, E. W. Understanding Asthma Using Animal Models. *Allergy Asthma Immunol. Res.* **2009**, *1*, 10–18.
29. Brewer, J. M.; Conacher, M.; Hunter, C. A.; Mohrs, M.; Brombacher, F.; Alexander, J. Aluminium Hydroxide Adjuvant Initiates Strong Antigen-Specific Th2 Responses in the Absence of Il-4-or Il-13-Mediated Signaling. *J. Immunol.* **1999**, *163*, 6448–6454.
30. Koike, E.; Takano, H.; Inoue, K.; Yanagisawa, R.; Kobayashi, T. Carbon Black Nanoparticles Promote the Maturation and Function of Mouse Bone Marrow-Derived Dendritic Cells. *Chemosphere* **2008**, *73*, 371–376.
31. Schinwald, A.; Murphy, F. A.; Jones, A.; MacNee, W.; Donaldson, K. Graphene-Based Nanoplatelets: A New Risk to the Respiratory System as a Consequence of Their Unusual Aerodynamic Properties. *ACS Nano* **2012**, *6*, 736–746.
32. Duch, M. C.; Budinger, G. R.; Liang, Y. T.; Soberanes, S.; Urich, D.; Chiarella, S. E.; Campochiaro, L. A.; Gonzalez, A.; Chandel, N. S.; Hersam, M. C.; *et al*. Minimizing Oxidation and Stable Nanoscale Dispersion Improves the Biocompatibility of Graphene in the Lung. *Nano Lett.* **2011**, *11*, 5201–5207.
33. Schinwald, A.; Murphy, F.; Askounis, A.; Koutsos, V.; Sefiane, K.; Donaldson, K.; Campbell, C. J. Minimal Oxidation and Inflammogenicity of Pristine Graphene with Residence in the Lung. *Nanotoxicology* **2014**, *8*, 824–832.
34. Wilson, J. W.; Li, X. The Measurement of Reticular Basement Membrane and Submucosal Collagen in the Asthmatic Airway. *Clin. Exp. Allergy* **1997**, *27*, 363–371.
35. Homer, R. J.; Elias, J. A. Airway Remodeling in Asthma: Therapeutic Implications of Mechanisms. *Physiology* **2005**, *20*, 28–35.
36. Ebina, M.; Takahashi, T.; Chiba, T.; Motomiya, M. Cellular Hypertrophy and Hyperplasia of Airway Smooth Muscles Underlying Bronchial-Asthma - a 3-D Morphometric Study. *Am. Rev. Respir. Dis.* **1993**, *148*, 720–726.
37. Carroll, N.; Cooke, C.; James, A. The Distribution of Eosinophils and Lymphocytes in the Large and Small Airways of Asthmatics. *Eur. Respir. J.* **1997**, *10*, 292–300.
38. Cockcroft, D. W.; Davis, B. E. Airway Hyperresponsiveness as a Determinant of the Early Asthmatic Response to Inhaled Allergen. *J. Asthma* **2006**, *43*, 175–178.
39. Dekkers, B. G.; Maarsingh, H.; Meurs, H.; Gosens, R. Airway Structural Components Drive Airway Smooth Muscle Remodeling in Asthma. *Proc. Am. Thorac. Soc.* **2009**, *6*, 683–692.
40. Cui, P.; Sharmin, S.; Okumura, Y.; Yamada, H.; Yano, M.; Mizuno, D.; Kido, H. Endothelin-1 Peptides and Il-5 Synergistically Increase the Expression of Il-13 in Eosinophils. *Biochem. Biophys. Res. Commun.* **2004**, *315*, 782–787.
41. Taneichi, M.; Naito, S.; Kato, H.; Tanaka, Y.; Mori, M.; Nakano, Y.; Yamamura, H.; Ishida, H.; Komuro, K.; Uchida, T. T Cell-Independent Regulation of IgE Antibody Production Induced by Surface-Linked Liposomal Antigen. *J. Immunol.* **2002**, *169*, 4246–4252.
42. Raes, G.; De Baetselier, P.; Noel, W.; Beschin, A.; Brombacher, F.; Hassanzadeh, G. Differential Expression of Fizz1 and Ym1 in Alternatively *versus* Classically Activated Macrophages. *J. Leukocyte Biol.* **2002**, *71*, 597–602.
43. Kzhyshkowska, J.; Mamidi, S.; Gratchev, A.; Kremmer, E.; Schmuttermaier, C.; Krusell, L.; Haus, G.; Utikal, J.; Schledzewski, K.; Scholtze, J.; *et al*. Novel Stabilin-1 Interacting Chitinase-Like Protein (Si-Clp) Is up-Regulated in Alternatively Activated Macrophages and Secreted *via* Lysosomal Pathway. *Blood* **2006**, *107*, 3221–3228.
44. Di Rosa, M.; De Gregorio, C.; Malaguarnera, G.; Tuttobene, M.; Biazzo, F.; Malaguarnera, L. Evaluation of Amcase and Chit-1 Expression in Monocyte Macrophages Lineage. *Mol. Cell. Biochem.* **2013**, *374*, 73–80.
45. Lee, C. G.; Da Silva, C. A.; Dela Cruz, C. S.; Ahangari, F.; Ma, B.; Kang, M. J.; He, C. H.; Takyar, S.; Elias, J. A. Role of Chitin and Chitinase/Chitinase-Like Proteins in Inflammation, Tissue Remodeling, and Injury. *Annu. Rev. Physiol.* **2011**, *73*, 479–501.
46. Neimert-Andersson, T.; Hallgren, A. C.; Andersson, M.; Langeback, J.; Zettergren, L.; Nilsen-Nygaard, J.; Draget, K. I.; van Hage, M.; Lindberg, A.; Gafvelin, G.; *et al*. Improved Immune Responses in Mice Using the Novel Chitosan Adjuvant Viscogel, with a Haemophilus Influenzae Type B Glycoconjugate Vaccine. *Vaccine* **2011**, *29*, 8965–8973.
47. Mogensen, T. H. Pathogen Recognition and Inflammatory Signaling in Innate Immune Defenses. *Clin Microbiol Rev.* **2009**, *22*, 240–273.
48. Da Silva, C. A.; Hartl, D.; Liu, W.; Lee, C. G.; Elias, J. A. Tlr-2 and Il-17a in Chitin-Induced Macrophage Activation and Acute Inflammation. *J. Immunol.* **2008**, *181*, 4279–4286.
49. Koller, B.; Muller-Wiefel, A. S.; Rupec, R.; Korting, H. C.; Ruzicka, T. Chitin Modulates Innate Immune Responses of Keratinocytes. *PLoS One* **2011**, *6*, e16594.
50. Chen, G. Y.; Yang, H. J.; Lu, C. H.; Chao, Y. C.; Hwang, S. M.; Chen, C. L.; Lo, K. W.; Sung, L. Y.; Luo, W. Y.; Tuan, H. Y.; *et al*. Simultaneous Induction of Autophagy and Toll-Like Receptor Signaling Pathways by Graphene Oxide. *Biomaterials* **2012**, *33*, 6559–6569.
51. Zhou, H. J.; Zhao, K.; Li, W.; Yang, N.; Liu, Y.; Chen, C. Y.; Wei, T. T. The Interactions between Pristine Graphene and Macrophages and the Production of Cytokines/Chemokines *via* Tlr- and Nf-Kappa B-Related Signaling Pathways. *Biomaterials* **2012**, *33*, 6933–6942.
52. Zhu, Z.; Zheng, T.; Homer, R. J.; Kim, Y. K.; Chen, N. Y.; Cohn, L.; Hamid, Q.; Elias, J. A. Acidic Mammalian Chitinase in Asthmatic Th2 Inflammation and Il-13 Pathway Activation. *Science* **2004**, *304*, 1678–1682.
53. Matsumoto, T.; Inoue, H.; Sato, Y.; Kita, Y.; Nakano, T.; Noda, N.; Eguchi-Tsuda, M.; Moriwaki, A.; Kan, O. K.; Matsumoto, K.; *et al*. Demethylallosamidin, a Chitinase Inhibitor, Suppresses Airway Inflammation and Hyperresponsiveness. *Biochem. Biophys. Res. Commun.* **2009**, *390*, 103–108.
54. De, M.; Chou, S. S.; Dravid, V. P. Graphene Oxide as an Enzyme Inhibitor: Modulation of Activity of Alpha-Chymotrypsin. *J. Am. Chem. Soc.* **2011**, *133*, 17524–17527.
55. Park, J. A.; Drazen, J. M.; Tschumperlin, D. J. The Chitinase-Like Protein YKL-40 Is Secreted by Airway Epithelial Cells at Base Line and in Response to Compressive Mechanical Stress. *J. Biol. Chem.* **2010**, *285*, 29817–29825.
56. Bara, I.; Ozier, A.; Girodet, P. O.; Carvalho, G.; Cattiaux, J.; Begueret, H.; Thumerel, M.; Ousova, O.; Kolbeck, R.; Coyle, A. J.; *et al*. Role of YKL-40 in Bronchial Smooth Muscle

Remodeling in Asthma. *Am. J. Resp. Crit. Care* **2012**, *185*, 715–722.
57. Homer, R. J.; Zhu, Z.; Cohn, L.; Lee, C. G.; White, W. I.; Chen, S.; Elias, J. A. Differential Expression of Chitinases Identify Subsets of Murine Airway Epithelial Cells in Allergic Inflammation. *Am. J. Physiol. Lung Cell Mol. Physiol.* **2006**, *291*, L502–511.
58. Konradsen, J. R.; James, A.; Nordlund, B.; Reinius, L. E.; Soderhall, C.; Melen, E.; Wheelock, A.; Carlsen, K. C. L.; Lidegran, M.; Verhoek, M.; *et al*. The Chitinase-Like Protein YKL-40: A Possible Biomarker of Inflammation and Airway Remodeling in Severe Pediatric Asthma. *J. Allergy Clin. Immun.* **2013**, *132*, 328–335.e5.
59. Drabner, B. Charakterisierung Und Identifizierung Von Immundominanten Bereichen Der L3-Chitinase Von Onchocerca Volvulus. [Ph.D. Thesis]. Humboldt University, Berlin, Germany, 2000.
60. Soukhtanloo, M.; Falak, R.; Sankian, M.; Varasteh, A. R. Generation and Characterization of Anti-Chitinase Monoclonal Antibodies. *Hybridoma* **2011**, *30*, 145–151.
61. Li, J.; Liu, Z.; Wu, Y.; Wu, H.; Ran, P. Chitosan Microparticles Loaded with Mite Group 2 Allergen Der F 2 Alleviate Asthma in Mice. *J. Invest. Allergol. Clin. Immunol.* **2008**, *18*, 454–460.
62. Kotchey, G. P.; Allen, B. L.; Vedala, H.; Yanamala, N.; Kapralov, A. A.; Tyurina, Y. Y.; Klein-Seetharaman, J.; Kagan, V. E.; Star, A. The Enzymatic Oxidation of Graphene Oxide. *ACS Nano* **2011**, *5*, 2098–2108.
63. Hsia, C. C. W.; Hyde, D. M.; Ochs, M.; Weibel, E. R. An Official Research Policy Statement of the American Thoracic Society/European Respiratory Society: Standards for Quantitative Assessment of Lung Structure. *Am. J. Resp. Crit. Care Med.* **2010**, *181*, 394–418.
64. Olmez, D.; Babayigit, A.; Erbil, G.; Karaman, O.; Bagriyanik, A.; Yilmaz, O.; Uzuner, N. Histopathologic Changes in Two Mouse Models of Asthma. *J. Invest Allergol. Clin. Immunol.* **2009**, *19*, 132–138.
65. Robbins, S. L.; Kumar, V.; Cotran, R. S. *Robbins and Cotran Pathologic Basis of Disease*, 8th ed.; Saunders/Elsevier: Philadelphia, PA, 2010; p xiv.
66. Maxie, M. G.; Jubb, K. V. F. *Pathology of Domestic Animals*, 5th ed.; Elsevier Saunders: Edinburgh, 2007.
67. Crissman, J. W.; Goodman, D. G.; Hildebrandt, P. K.; Maronpot, R. R.; Prater, D. A.; Riley, J. H.; Seaman, W. J.; Thake, D. C. Best Practices Guideline: Toxicologic Histopathology. *Toxicol. Pathol.* **2004**, *32*, 126–131.
68. Trott, O.; Olson, A. J. Autodock Vina: Improving the Speed and Accuracy of Docking with a New Scoring Function, Efficient Optimization, and Multithreading. *J. Comput. Chem.* **2010**, *31*, 455–461.